Polym. Korea, Vol. 44, No. 4, pp. 519-526 (2020)
https://doi.org/10.7317/pk.2020.44.4.519

ISSN 0379-153X(Print)
ISSN 2234-8077(Online)

Sulfur/Accelerator 비율이 천연고무 인장특성 및 구조불균형에 미치는 영향 연구

Abdulhakim Masa†, Siriwat Soontaranon*, and Nabil Hayeemasae**

Sino-Thai International Rubber College, Prince of Songkla University
*Synchrotron Light Research Institute
**Department of Rubber Technology and Polymer Science, Faculty of Science and Technology, Prince of Songkla University

(2020년 3월 14일 접수, 2020년 4월 16일 수정, 2020년 4월 22일 채택)

Influence of Sulfur/Accelerator Ratio on Tensile Properties and Structural Inhomogeneity of Natural Rubber

Abdulhakim Masa†, Siriwat Soontaranon*, and Nabil Hayeemasae**

Sino-Thai International Rubber College, Prince of Songkla University, Hat Yai, Songkhla 90110, Thailand
**Synchrotron Light Research Institute, Muang District, Nakhon Ratchasima 30000, Thailand*
***Department of Rubber Technology and Polymer Science, Faculty of Science and Technology, Prince of Songkla University, Pattani Campus, Pattani 94000, Thailand*

(Received March 14, 2020; Revised April 16, 2020; Accepted April 22, 2020)

Abstract: Sulfur and accelerators play very important roles in curing natural rubber, influencing the properties of rubber vulcanizates. Such properties are also associated with the microstructure of vulcanized natural rubber. In this study, the relationships between tensile properties, strain-induced crystallization behavior, and structural inhomogeneity were investigated with special attention to the ratio of sulfur to accelerator (S/Acc). Increasing the S/Acc ratio increased crosslink density, simply from having more of the crosslinking agent. The highest tensile strength was obtained at unit ratio (=1), which was associated with SIC behavior based on wide angle x-ray diffraction measurements. Reductions in both the tensile strength and crystallinity were noticed when the crosslink density was relatively high. Structural inhomogeneity of network structures induced by crosslinking was investigated by means of small angle x-ray scattering, which showed the increased size and improved homogeneity of distribution with increased S/Acc ratio.

Keywords: natural rubber, tensile properties, microstructure, strain-induced crystallization.

Introduction

Vulcanization is a well-known action that turns the viscous and elastic rubber materials into versatile and elastic materials in the presence of crosslink agent and heat. Among crosslinking agents used in rubber compounding, sulfur was found to be the foremost extensively utilized in the rubber industries due to its efficiency, loosely compatible with compounding ingredients, and permits to predict the ultimate vulcanizate properties.[1] In general, sulfur vulcanization systems are classified into three systems, depending on sulphur/accelerator (S/Acc) ratio. High S/Acc ratio, e.g., 1.67 to 8.75 is called conventional vulcanization (CV). Moderate S/Acc ratio (0.42-1.42) refers as the semi-efficient vulcanization (Semi-EV), and low S/Acc ratio (0.08 to 0.4) is labeled as efficient vulcanization (EV).[2] Each system provides its own advantages depending on the designed formulation of rubber compounders.

Natural rubber (NR) is extensively used in the rubber industries and is mostly vulcanized in the presence of sulfur. This type of rubber exhibits excellent and uncommon mechanical properties. These exceptional properties combine high tensile strength, elongation at break and good crack growth resistance, and these are partly associated with the ability of rubber to crystallize under stretching, which is known as strain-induced crystallization (SIC).[3,4] The crystallites generated by SIC are believed to act as additional filler or as crosslinks,[5,6] so the rubber can self-reinforce without added reinforcing filler. Thus, the SIC behavior is an important factor contributing to the mechanical properties of NR.

†To whom correspondence should be addressed.
abdulhakim.m@psu.ac.th, ORCID 0000-0002-0577-4844

The SIC of NR has been extensively studied, and the mechanisms of SIC have been elaborated in some detail.[7] It is believed that the shorter chains are the first ones to be fully stretched, and subsequently act as nucleation sites for crystallites. Various factors have been reported to affect the mechanical properties and crystallization behaviour of NR. In unfilled vulcanizate, crosslink density is a very important parameter dominating in various final properties of the products.[8-10] Zhao *et al*.[9] demonstrated that the mechanical properties, namely hardness, 300% modulus, tensile strength, and elongation at break strongly depend on crosslink density. Similar observations were reported by authors.[8,10] The effects of crosslink density on SIC are also discussed in literature.[7,11-14] Trabelsi *et al*.,[11] investigated the effects of crosslink density on properties and crystallization behaviour of NR, by using three sulfur contents (0.8, 1.2, and 2 phr). They found that the crystallinity and crystallization rate both decreased with crosslink density. Furthermore, they also noticed decreased crystallite size with increased crosslink density. Later on, Chenal *et al*.,[12,13] investigated the effects of crosslink density in NR on the crystallization rate during stretching. They reported that the crystallization rate increased when the crosslink density was below 1.2×10^{-4} mol.cm^{-3}. Crosslink densities beyond 1.2×10^{-4} mol.cm^{-3} decreased the crystallization rate. The former characteristic was attributed to the nucleation of crystallites, while the latter was governed by the growth of the crystallites in uniaxial deformation. In conflict with this, Tosaka *et al*.,[7] found that both crystallinity and crystallization rate increased with crosslink density. So, while the influences of crosslink density on SIC behaviour have been extensively studied, the results do not show a consistent pattern. Furthermore, the effects of crosslink density on structural inhomogeneity (size and distribution) of crosslinked network structures has not been discussed previously. Therefore, it is necessary to further explore the effects of crosslink density on mechanical properties and on microstructural changes in crosslinked NR. The NR samples with various crosslink densities were prepared by using different sulfur and accelerator ratios. The changes in crosslink density was studied by means of swelling tests. Tensile properties and corresponding microstructural changes during stretching were studied by means of tensile-testing and wide angle x-ray diffraction (WAXD), and sizes as well as distributions of crosslinked network structures were revealed by small angle x-ray scattering (SAXS) measurements. This study contributes to the scientific understanding on how sulfur and accelerators influence the microstructure in a rubber vulcanizate, and provide useful information for predicting the performance of natural rubber.

Experimental

Materials. NR grade STR 5L was purchased from Chalong Concentrated Natural Rubber Latex Industry Co., Ltd., Thailand. Stearic acid and zinc oxide (ZnO) were manufactured by Imperial Chemical Co. Ltd., Pathumthani, Thailand and Global Chemical Co. Ltd., Samut Prakarn, Thailand, respectively, and these were used as activators. *N*-cyclohexyl-benzothiazyl-sulphenamide (CBS) used as accelerator was purchased from Flexsys America L.P., West Virginia, USA, and sulfur used as crosslinking agent was supplied by Siam Chemical Co., Ltd., Samut Prakan, Thailand.

Sample Preparation. NR and other ingredients such as stearic acid, ZnO, CBS and sulfur were compounded in a laboratory-sized internal mixer (Brabender® GmbH & Co. KG, Duisburg, Germany). The compound formulations and mixing steps are displayed in Table 1. Total mixing time was kept constant at 5 min and total compounding ingredients were fixed at 107 part(s) per hundred parts of rubber (phr) for all samples. The compounds were compression molded by hot pressing at 160 °C each for its respective curing time determined with a rheometer. In this study, the amounts of curative and accelerator were varied, but the total of curative and its accelerator was held fixed at 3 phr. The samples with S/Acc ratios of 0.07, 0.2, 0.5, 1 and 2 were labelled as S0.07, S0.2, S0.5, S1 and S2, respectively.

Characterizations. Curing Characteristics: The curing characteristics of the NR compounds with varied S/Acc ratios were investigated at 160 °C using a moving die rheometer (Montech MDR 3000 BASIC, Germany). The scorch time

Table 1. Compound Formulations and Mixing Schedules for NR with Various S/Acc Ratios

Ingredient	Quantity (phr)					Mixing time (min)
	S0.07	S0.2	S0.5	S1	S2	
NR	100	100	100	100	100	2
Stearic acid	1	1	1	1	1	1
ZnO	3	3	3	3	3	
CBS	2.8	2.5	2	1.5	1	1
S	0.2	0.5	1	1.5	2	1
S/Acc ratio	0.07	0.2	0.5	1	2	Dump at 5 min

(t_{s1}), cure time (t_{c90}), maximum torque (M_H) and torque difference (M_H-M_L) were determined.

Swelling Measurement: The swelling test was performed to estimate the crosslink density (ν) in each vulcanizate sample. The rubber specimens were immersed in toluene solvent at room temperature for 168 h. The solvent was refreshed every 24 h. The swelling percentage was calculated as follows.

$$\text{Swelling } (\%) = \left(\frac{W_s - W_i}{W_i}\right) \times 100 \quad (1)$$

where W_i is the initial weight of sample (g) and W_s is the weight of swollen sample (g). The results from the swelling test were used to estimate the crosslink density (ν) in each NR vulcanizate by applying the Flory-Rehner equation:[15]

$$\nu = \frac{1}{2M_c} = -\frac{\ln(1-V_r) + V_r + \chi V_r^2}{2\rho V_s\left(V_r^{1/3} - \frac{V_r}{2}\right)} \quad (2)$$

where V_r is the volume fraction of rubber in the swollen mass, χ is the polymer-solvent interaction parameter (0.39 for the NR-toluene system),[16] ρ is density of the polymer, and V_s is molar volume of the solvent (106.3 cm^3/mol). The V_r can be calculated from eq. (3):

$$V_r = \frac{\frac{W_1}{\rho_r}}{\frac{W_1}{\rho_r} + \frac{(W_2 - W_1)}{\rho_s}} \quad (3)$$

where W_1 is de-swollen weight, W_2 is swollen weight, ρ_r is density of rubber, and ρ_s is density of toluene.

Tensile Measurement: The tensile properties of NR vulcanizates were investigated by means of a universal tensile testing machine (LLOYD Instruments, LR5K Plus, UK). Dumbbell shaped test specimens were cut and tested at room temperature and 500 mm/min crosshead speed according to ISO 37. Five replicates were done for each type of sample in the tensile test.

WAXD and SAXS Measurement: Crystallization behaviors under stretching of the NR vulcanizates were investigated by means of WAXD, while the structural inhomogeneity, including size and distribution of crosslinked networks were estimated by means of SAXS measurements. Both WAXD and SAXS were performed at Beamline 1.3 W, the Siam Photon Laboratory, Synchrotron Light Research Institute (SLRI), Nakhon-Ratchasima, Thailand. The distance from sample to detector was 11.5 cm for WAXD, and 4.5 m for SAXS. The WAXD and SAXS data were collected during continuous stretching with a crosshead speed of 50 mm/min, and the exposure time for collecting data at a fixed strain was about 30 sec. All WAXD and SAXS data were normalized and corrected by using SAXSIT data processing software.

Results and Discussion

Curing Characteristics. The curing characteristics in term of t_{s1}, t_{c90}, M_H and M_H-M_L at 160 °C of the NR compounds with varied S/Acc ratios is shown in Table 2. The t_{s1} and t_{c90} decreased slightly with increasing S/Acc ratio, shorter t_{s1} and t_{c90} indicates faster curing process. This is extremely beneficial as they increase the production rate. However, an increase of both t_{s1} and t_{c90} was again noticed at S/Acc equal to 2, where the accelerator content was too low due to an insufficient amount of accelerator for the curing reactions. This is commonly observed as lower content of accelerator was used in the formulation.[8,17,18] It was observed that the M_H and M_H-M_L increased with increasing the ratio S/Acc. The M_H is a measure of stiffness of the compounds while the M_H-M_L indicates the degree of crosslinking.[19] This has suggested that the stiffness and crosslinking degree of the vulcanizates increased as the ratio of S/Acc increased. A higher loading of the sulfur crosslinking agent induces a greater crosslink density due to the higher availability of active sulfurating agents for crosslinking.

Table 2. Cure Characteristics at 160 °C of the NR Compounds with Varied S/Acc Ratios

Samples	Curing characteristics			
	t_{s1} (min)	t_{c90} (min)	M_H (dN.m)	M_H-M_L (dN.m)
S2	1.05 ± 0.01	2.48 ± 0.13	22.19 ± 0.10	18.73 ± 0.11
S1	0.85 ± 0.00	1.73 ± 0.01	20.86 ± 0.54	17.50 ± 0.60
S0.5	0.94 ± 0.02	1.94 ± 0.01	20.47 ± 0.20	17.13 ± 0.14
S0.2	0.87 ± 0.06	1.94 ± 0.09	19.17 ± 0.23	15.54 ± 0.17
S0.07	1.03 ± 0.01	2.84 ± 0.05	14.36 ± 0.40	10.97 ± 0.34

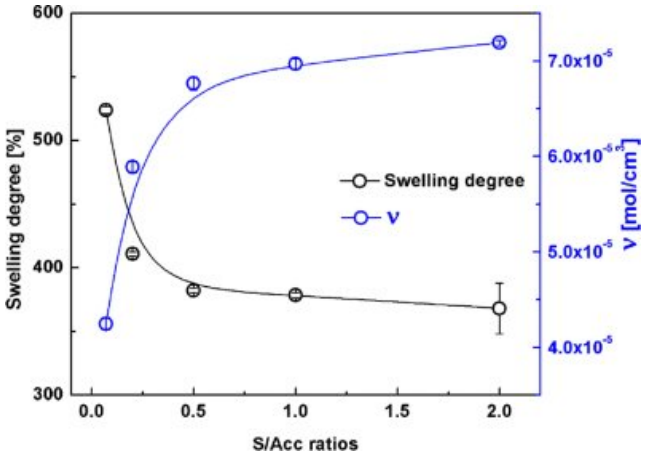

Figure 1. Degree of swelling and crosslink density of NR compounds with various S/Acc ratios.

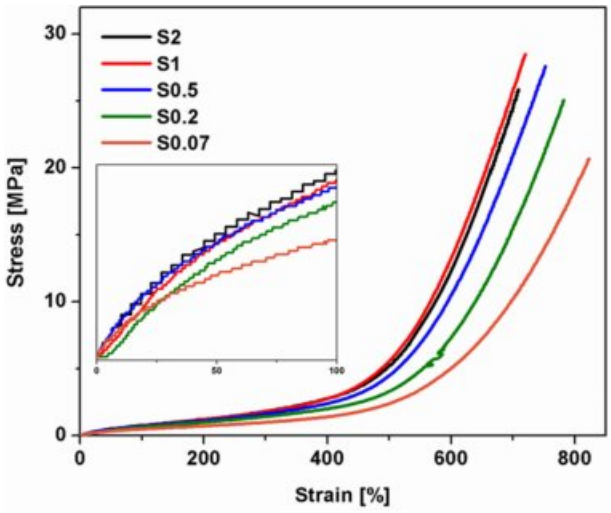

Figure 2. Stress-strain curves of NR vulcanizates with various S/Acc ratios.

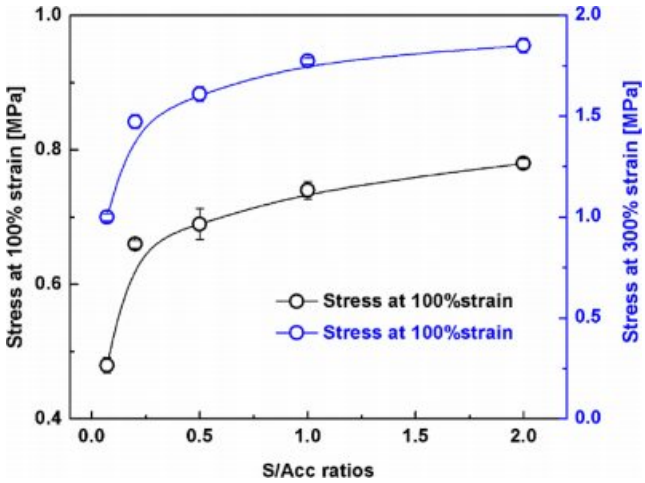

Figure 3. Stress at 100% and 300% strains of NR vulcanizates with various S/Acc ratios.

Swelling Behavior. Figure 1 shows the degree of swelling in NR crosslinked with the various S/Acc ratios. The swelling of NR vulcanizates decreased with S/Acc ratio, implying lesser solvent penetration into the samples. It is well-known that the swelling capacity is inversely related to the total crosslink density, and a lower swelling degree indicates a higher crosslink density.[19] The crosslink density (ν) in the various samples was later estimated by applying the Flory-Rehner equation,[15] and the results are also included in Figure 1. In accordance with curing characteristics results, the crosslink density in NR increased with S/Acc ratio. The highest ν was obtained for the highest concentration of sulfur (S/Acc = 2). Increase of crosslink density with S/Acc ratio was due to the increased sulfurating chemicals causing initiation and propagation of the crosslinking reactions. Thus, crosslink density increased with the S/Acc ratio.

Tensile Properties. Figure 2 shows stress-strain curves of NR vulcanizates with the various S/Acc ratios. It is seen that all curves showed a steep increase in stress at high strains (i.e., over 400% strains) and this pattern in response was attributed to the SIC behavior.[20,21] It is also seen that the stress at low strain also increased with S/Acc ratio (see the embedded Figure) due to crosslink density.[9]

The stress at 100% and 300% strains, tensile strength and elongation at break are shown in Figures 3 and 4. Figure 3 shows the stresses at 100% and 300% strains for the NR vulcanizates with varied S/Acc ratios. Both stresses increased gradually with S/Acc ratio, which is again attributed to crosslinking density. A higher crosslink density gives a stronger network and thus enhances the stress at 100% and 300% strains.

Figure 4 shows tensile strength and elongation at break of the NR vulcanizates. The tensile strength increased passing through a maximum as S/Acc ratio increased. The highest tensile strength was obtained at S/Acc equal to 1, with the crosslink density approximately 7×10^{-5} mol/cm^3. Reduction of tensile strength after the maximum was attributed to excessive crosslink density. When the crosslink density is relatively high, the chain length between two adjacent crosslinking points is short, restricting orientation of the chains during stretching; thus the tensile strength decreases.[9,22] The elongation at break decreased with S/Acc ratio because stiffness of the rubber increased with crosslink density, restricting rubber chain mobility.

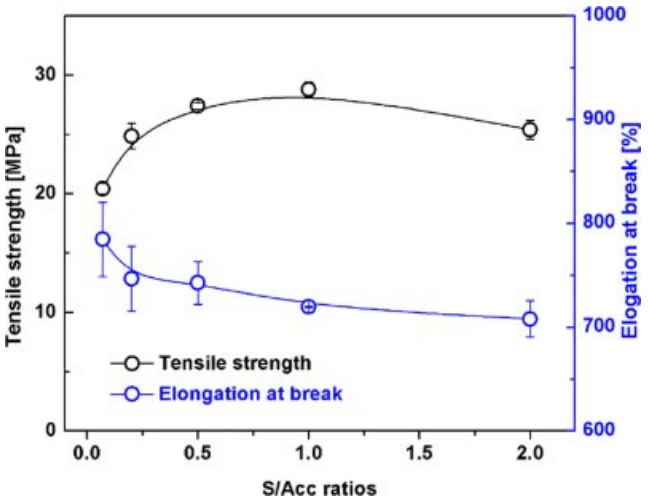

Figure 4. Tensile strength and elongation at break of NR vulcanizates with various S/Acc ratios.

Based on the tensile testing, increased crosslink density was responsible for increasing stress at 100% and 300% strains, while the tensile response from SIC occurs at higher strains. SIC provides self-reinforcement to vulcanized rubber.[4,23] Therefore, crystallization behavior during stretching should be given attention. To gain further understanding of the effects of S/Acc ratio on high strain tensile behaviors, WAXD measurements were conducted during tensile deformation.

WAXD and SAXS. Figure 5 shows representative 2D WAXD images of unstretched (0% strain) and highly stretched states (505% strain) of vulcanized samples, and the linear 1D data at highly stretched state are also included. Without deformation, no reflection spots were observed in the 2D image and the corresponding 1D pattern appeared as the blue line (amorphous pattern). In a highly deformed state, reflection spots were detected in the 2D image and a crystalline peak appeared in the corresponding 1D pattern (black line). After peak fitting with SAXSIT software, the areas of amorphous and crystalline peaks were recorded. Among the diffraction spots, the crystallographic planes (200) and (120) are of particular importance. In this study, variation of the crystallinity and crystallite size corresponding to (200) plane was assessed during deformation.

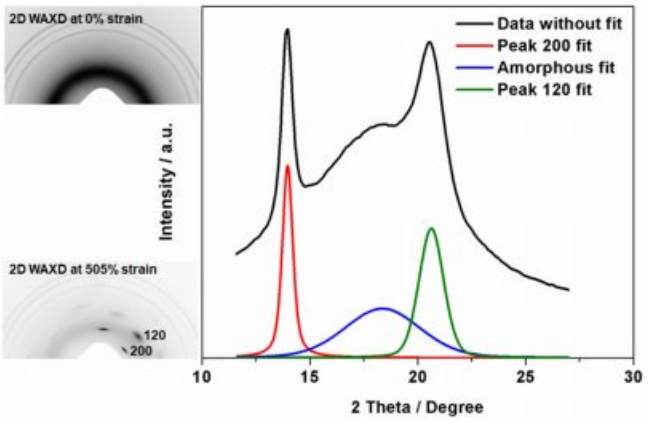

Figure 5. Representative 2D WAXD images and 1D data in unstretched and highly stretched states (sample S/Acc = 2).

Figure 6 shows a plot of (A) degree of crystallinity (%), and (B) of lateral crystallite size corresponding to (200) plane, during stretching of the NR vulcanizates with various S/Acc ratios. The degree of crystallinity (DC) was calculated as follows;[24]

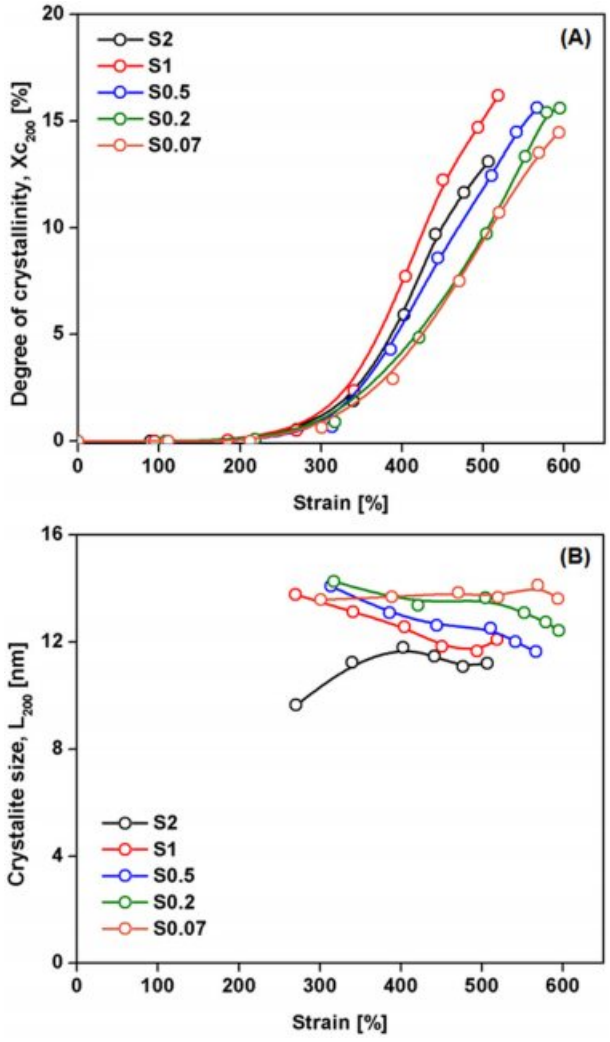

Figure 6. Plot of (A) degree of crystallinity (%); (B) lateral crystallite size corresponding to the (200) plane during stretching of the NR vulcanizates with various S/Acc ratios.

$$DC = \frac{A_c}{A_c + A_a} \times 100 \quad (4)$$

Here, A_c is the area of crystalline peaks assigned to the (200) plane, and A_a is the area of the amorphous halo.

The Scherrer equation was used to estimate the average crystallite size in the direction perpendicular to the (200) plane (L_{200}) as follows:[25,13]

$$L_{200} = \frac{K\lambda}{\beta \cos\theta} \quad (5)$$

where the K is 0.89, λ is the wavelength, β is the half-width at half-height, and θ is the Bragg angle.

As can be seen from Figure 6(A), the crystallinity in all cases increased with strain, because stretching oriented the rubber chains. It is believed that initially SIC originates from highly stretched short chain segments between crosslinks that are heterogeneously distributed. The shorter chains are fully stretched and became nucleation sites for crystallites.[24] These crystallites behave as filler or additional crosslinks,[5,6] providing self-reinforcement to the rubber, and thus stress increases rapidly at high tensile strains. It is also seen that the crystallinity at any given strain increased with S/Acc ratio (via the crosslink density), and the highest crystallinity was found for S/Acc ratio equal to 1. It should be mentioned that the rate of crystallization seemed to increase with S/Acc ratio, except that the crystallization rate was decreased at ratio 2. This result suggests that the best choice of S/Acc is about 1. Further increase in S/Acc reduced the SIC effects due to excessive crosslinking that hindered crystallization.[26] The variation of crystallinity corresponds well to the stress-strain curves (Figure 2), so the tensile properties can be partly explained by the SIC behavior.

Figure 6(B) shows two interesting phenomena regarding the crystallite size during stretching. When the ratio of S/Acc was 2, and the crosslink density is excessive, the crystal size developed from small to large while other cases showed opposite behavior. Moreover, the size of crystals was also smaller than in the other cases at any given strain. These observations can be explained by two mechanisms: 1) the large amount of short chains serving as crystallite nucleation is favored in the sample containing high crosslink density. When the crystal formed in the densely crosslink area, high number of crystal formation suppressed each other and thus the size of crystal becomes small; and 2) when the crosslink density was high, the molecular chains between crosslinks were short. Shortening the free segments of molecular chains suppresses chain mobility and orientation responses that produce large crystallites during stretching,[11,24] while the crystallite size in less crosslinked rubber sample was larger due to the longer free chains between crosslinks.[11]

To assess the network structures in the samples with various S/Acc ratios, SAXS measurements were conducted. Figure 7 shows plot of $I(q)$ as a function of q for the NR samples with various S/Acc ratios. $I(q)$ is the scattering intensity at q, and q is the scattering vector ($q = (4\pi/\lambda) \sin\theta$, where λ and 2θ is the wavelength and scattering angle). Owing to the vulcanizates contained various elements, e.g., ZnO, sulfur and other impurities in NR, argument of these elements affected electron density fluctuations in the SAXS patterns may arise. However, it has been reported that the ZnO particles do not contribute to the SAXS patterns, due to the micrometer size range that is not contributing the small q range, and the SAXS intensity patterns for uncrosslinked rubber compound containing sulfur displayed lower intensity than that for crosslinked sample.[27] Therefore, the effects of ZnO, unreacted sulfur and others components (including impurities) can be ignored and the pattern of SAXS after vulcanization should be attributed to crosslinked networks. The crosslinking reactions changed the local electron density at the crosslink and in its neighborhood, and can be detected by SAXS.

From Figure 7, it is clearly seen that all cases showed an upturn in intensity within the low-q region, caused by the heterogeneous network structures in the vulcanizates created by chemical crosslinking.[28,29] Interestingly, the intensity decreased with S/Acc ratio (or with crosslink density), indicating

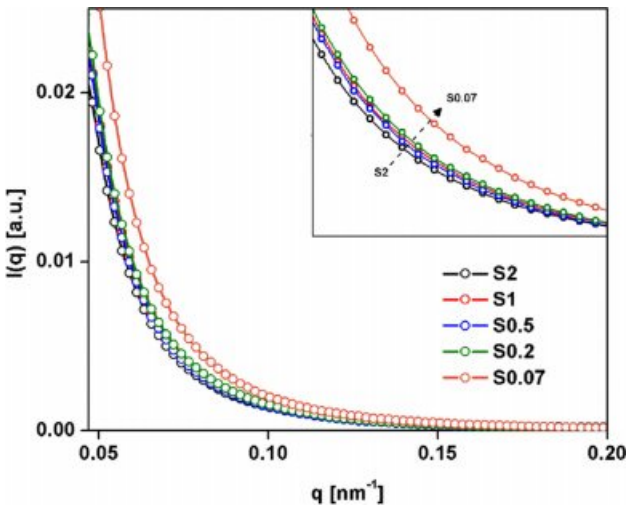

Figure 7. Linear SAXS patterns of NR vulcanizates with various S/Acc ratios.

decreasing heterogeneity.[28] Increasing the crosslink density improved homogeneity of networks in the rubber vulcanizates. Previously it has been suggested that excessive crosslinking may create inhomogeneous network structures, although no convincing evidence was provided.[30] Within the range of S/Acc ratios in recent studies, the SAXS results suggest that increasing crosslink density improved homogeneity, so the inhomogeneity of crosslinks should not be responsible for cracks in highly crosslinked specimens. The cracks in highly crosslinked sample will be discussed later.

In addition to the distribution of network structures, the characteristic size of crosslinked structures formed during vulcanization is another factor contributing to the SAXS profile. The characteristic size of crosslinked network structures can be estimated by applying the Debye-Bueche equation:[31,32]

$$I(q) = \frac{I(0)}{(1+\Xi^2 q^2)^2} \quad (6)$$

where Ξ is the characteristic size of the heterogeneous network structures.

Figure 8 shows the characteristic size of the crosslinked structures in the various vulcanizate samples. The characteristic size increased with S/Acc ratio, suggesting that the size of crosslinked networks became larger as the crosslink density increased. This might be attributed to the greater number of crosslink agents readily available for crosslinking reactions.

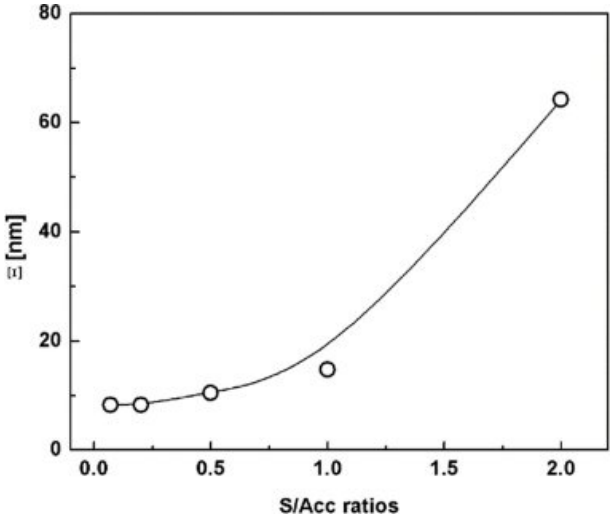

Figure 8. Characteristic sizes (Ξ) of the heterogeneous network structures in NR vulcanizates with various S/Acc ratios.

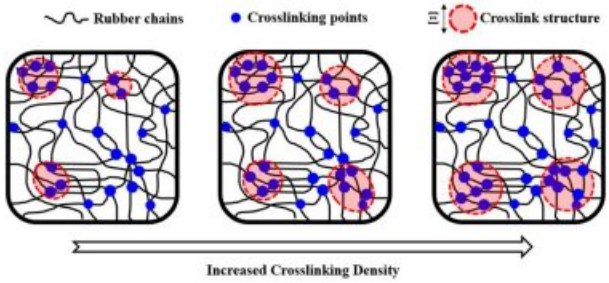

Figure 9. Illustration of crosslinked network structure changes with crosslink density.

Increase of characteristic size of crosslinked structures with increment of crosslink agent was also reported previously, based on small-angle neutron scattering.[29] It is interesting that large-sized crosslinked networks contain lots of crosslinks and thus the number of short free chains would be also high. These short chains would then limit the extension and orientation of molecular chains around the crosslink junctions during deformation, and cracking could be initiated where the short chains are dense. This could be the mechanism of crack formation with high crosslink density.

Based on the WAXD and SAXS results, a model illustration of how crosslink density influences size and homogeneity of the network structures could be developed, and is shown in Figure 9. When the crosslink density is small, inhomogeneity of the network sizes would be seen initially, as a result of high competition for the reactive sites on rubber chains to interact with a small amount of crosslinking agents. Increasing the amount of crosslinking agents reduced competition between the active chains for reacting with the sulfur crosslinking agents, thus increasing the size of crosslinked structures with less heterogeneity.

Improved homogeneity of the crosslinked network structures contributed to SIC. However, the size of network structure also increased with the ratio S/Acc. Large size of the crosslinked network structures may have negative effects on the crystallization in NR and tensile properties, as suggested by the highest S/Acc ratio in this current study. Therefore, the mechanical properties of rubber vulcanizates depend on various factors, including crosslink density, distribution and size of network structures, and their ability to crystallize during stretching. Carefully selecting the proper balance between sulfur and its accelerator could improve the mechanical properties of vulcanizates.

Conclusions

In this study, effects of various sulfur to accelerator (S/Acc) ratios, ranging from 0.07 to 2.0, on swelling and mechanical properties, and structure inhomogeneity of NR vulcanizates were investigated. Increasing the S/Acc ratio usually increased maximum torque, torque difference and crosslink density, because there was more crosslinking agent in the compound. Stress at low strains also increased with the S/Acc ratio, but the highest tensile strength was obtained when the ratio was 1 and the crosslink density was about 7×10^{-5} mol/cm^3. Deformation induced crystallization was assessed by means of WAXD and it matched well the observed tensile strengths. It is interesting to note that the crystallite size developed from small to big in the sample where the crosslink density was the highest among those tested. Furthermore, the sizes of crosslinked network structures were found to increase, with a more homogeneous distribution, when the ratio S/Acc (or the crosslink density) was increased. Based on SAXS measurements both these structural parameters played important roles in crystallization and in tensile strength of the NR vulcanizates.

Acknowledgements: The authors gratefully acknowledged Prince of Songkla University for financial support (Grant No. RDO6202102S). Research and Development Office (RDO), Prince of Songkla University and Assoc. Prof. Dr. Seppo Karrila are also acknowledged for assistance in editing the English language in this manuscript.

References

1. P. A. Ciullo and N. Hewitt, *The Rubber Formulary*, William Andrew, New York, 1999.
2. R. N. Datta, *Rubber Curing Systems*, Smithers Rapra Technology, Shawbury, 2002.
3. K. Bruning, K. Schneider, S. V. Roth, and G. Heinrich, *Polymer,* **54**, 6200 (2013).
4. Y. Fukahori, *Polymer*, **51**, 1621 (2010).
5. B. Huneau, *Rubber Chem. Technol.*, **84**, 425 (2011).
6. M. Tosaka, K. Senoo, S. Kohjiya, and Y. Ikeda, *J. Appl. Phys.*, **101**, 084909 (2007).
7. M. Tosaka, S. Kohjiya, S. Murakami, S. Poompradub, Y. Ikeda, S. Toki, I. Sics, and B. S. Hsiao, *Rubber Chem. Technol.*, **77**, 711 (2004).
8. L. Gonzalez, A. Rodriguez, J. L. Valentin, A. Marcos-Fernandez, and P. Posadas, *Kautschuk und Gummi Kunststoffe*, **58**, 638 (2005).
9. F. Zhao, W. Bi, and S. Zhao, *J. Macromol. Sci. B*, **50**, 1460 (2011).
10. K. Boonkerd, C. Deeprasertkul, and K. Boonsomwong, *Rubber Chem. Technol.*, **89**, 450 (2016).
11. S. Trabelsi, P. A. Albouy, and J. Rault, *Macromolecules*, **36**, 7624 (2003).
12. J. M. Chenal, C. Gauthier, L. Chazeau, L. Guy, and Y. Bomal, *Polymer*, **48**, 6893 (2007).
13. J. M. Chenal, L. Chazeau, L. Guy, Y. Bomal, and C. Gauthier, *Polymer*, **48**, 1042 (2007).
14. Z.-T. Xie, M.-C. Luo, C. Huang, L.-Y. Wei, Y.-H. Liu, X. Fu, G. Huang, and J. Wu, *Polymer*, **151**, 279 (2018).
15. P. J. Flory and J. Rehner, Jr., *J. Chem. Phys.*, **11**, 512 (1943).
16. S. Musto, V. Barbera, V. Cipolletti, A. Citterio, and M. Galimberti, *Express Polym. Lett.*, **11**, 435 (2017).
17. B. H. Park, I. G. Jung, and S. S. Park, *Polym. Korea*, **25**, 63 (2001).
18. S. Rabiei and A. Shojaei, *Eur. Polym. J.*, **81**, 98 (2016).
19. H. Nabil, H. Ismail, and A. R. Azura, *J. Vinyl Addit. Technol.*, **21**, 79 (2015).
20. A. Masa, R. Saito, H. Saito, T. Sakai, A. Kaesaman, and N. Lopattananon, *J. Appl. Polym. Sci.*, **133**, 43214 (2016).
21. M. Tosaka, *Polym. J.*, **39**, 1207 (2007).
22. G. R. Hamed and N. Rattanasom, *Rubber Chem. Technol.*, **75**, 935 (2002).
23. B. Ozbas, S. Toki, B. S. Hsiao, B. Chu, R. A. Register, I. A. Aksay, R. K. Prudhomme, and D. H. Adamson, *J. Polym. Sci., Part B: Polym. Phys.*, **50**, 718 (2012).
24. M. Tosaka, S. Murakami, S. Poompradub, S. Kohjiya, Y. Ikeda, S. Toki, I. Sics, and B. S. Hsiao, *Macromolecules*, **37**, 3299 (2004).
25. Y. Ikeda, Y. Yasuda, K. Hijikata, M. Tosaka, and S. Kohjiya, *Macromolecules*, **41**, 5876 (2008).
26. E. H. Andrews, *J. Polym. Sci., Part B: Polym. Phys.*, **4**, 668 (1966).
27. W. Salgueiro, A. Somoza, I. L. Torriani, and A. J. Marzocca, *J. Polym. Sci., Part B: Polym. Phys.*, **45**, 2966 (2007).
28. N. Osaka, M. Kato, and H. Saito, *J. Appl. Polym. Sci.*, **129**, 3396 (2013).
29. Y. Ikeda, N. Higashitani, K. Hijikata, Y. Kokubo, Y. Morita, M. Shibayama, N. Osaka, T. Suzuki, H. Endo, and S. Kohjiya, *Macromolecules*, **42**, 2741 (2009).
30. W. Sainumsai, S. Toki, S. Amnuaypornsri, A. Nimpaiboon, J. Sakdapipanich, L. Rong, B. S. Hsiao, and K. Suchiva, *Rubber Chem. Technol*., **90**, 728 (2017).
31. P. Debye and A. M. Bueche, *J. Appl. Phys.*, **20**, 518 (1949).
32. A. Izumi, Y. Shudo, T. Nakao, and M. Shibayama, *Polymer*, **103**, 152 (2016).